AGU PUBLICATIONS

Geophysical Research Letters

RESEARCH LETTER
10.1002/2016GL072023

Key Points:
- The changes in sea surface temperature, surface fluxes and clouds induced by tropical cyclones are determined from observations and a model
- Subtropical regions can exhibit strong regional variations in TC-induced SST change, based on local oceanic features and low-level clouds
- Results point to potential connections between TCs, ocean temperature, and low-cloud distributions that can influence tropical heat budgets

Supporting Information:
- Supporting Information S1

Correspondence to:
R. L. Sriver,
rsriver@illinois.edu

Citation:
Huang, A., H. Li, R. L. Sriver, A. V. Fedorov, and C. M. Brierley (2017), Regional variations in the ocean response to tropical cyclones: Ocean mixing versus low cloud suppression, *Geophys. Res. Lett.*, *44*, doi:10.1002/2016GL072023.

Received 18 NOV 2016
Accepted 7 FEB 2017
Accepted article online 9 FEB 2017

Regional variations in the ocean response to tropical cyclones: Ocean mixing versus low cloud suppression

Andrew Huang[1], Hui Li[1], Ryan L. Sriver[1], Alexey V. Fedorov[2], and Chris M. Brierley[3]

[1]Department of Atmospheric Sciences, University of Illinois at Urbana-Champaign, Urbana, Illinois, USA, [2]Department of Geology and Geophysics, Yale University, New Haven, Connecticut, USA, [3]Department of Geography, University College London, London, UK

Abstract Tropical cyclones (TCs) tend to cool sea surface temperature (SST) via enhanced vertical mixing and evaporative fluxes. This cooling is substantially reduced in the subtropics, especially in the northeastern Pacific where the occurrence of TCs can warm the ocean surface. Here we investigate the cause of this anomalous warming by analyzing the local oceanic features and TC-induced anomalies of SST, surface fluxes, and cloud fraction using satellite and in situ data. We find that TCs tend to suppress low clouds at the margins of the tropical ocean warm pool, enhancing shortwave radiative surface fluxes within the first week following storm passage, which, combined with spatial variations in ocean thermal structure, can produce a ~1°C near-surface warming in the northeastern Pacific. These findings, supported by high-resolution Earth system model simulations, point to potential connections between TCs, ocean temperature, and low cloud distributions that can influence tropical surface heat budgets.

1. Introduction

Tropical cyclones (TCs) are extreme weather events that can alter the vertical structure of the upper ocean, through intense fluxes of heat and momentum at the ocean-atmosphere interface. The ocean response to TCs is typically characterized by surface cooling along storm wakes [*Price*, 1981], along with warming beneath the mixed layer associated with the redistribution of ocean heat by vertical mixing [*Mei et al*., 2013; *Cheng et al.,* 2015]. The cool surface conditions typically persist for several days to weeks, while the subsurface warming can persist for several months or longer. TC-induced ocean warm anomalies can be advected away from storm regions by large-scale currents [*Pasquero and Emanuel*, 2008; *Manucharyan et al.,* 2011; *Bueti et al.,* 2014) or reabsorbed by the mixed layer (and then damped by the atmosphere) on interseasonal timescales [*Jansen et al.,* 2010].

Past studies have shown that the aggregated effects of TC-induced ocean heat anomalies can have potentially important implications for tropical ocean mixing and heat budgets [*Sriver and Huber*, 2007; *Sriver et al.,* 2010], which may influence global climate variability on a wide range of timescales. For example, variability in basin-aggregated TC-induced ocean heat anomalies can influence hemispheric atmospheric circulations and weather patterns on seasonal timescales [*Sriver and Huber*, 2010; *Hart*, 2011]. TCs may also be important for characterizing variations in global ocean-atmosphere energy budgets and ocean heat transport [*Emanuel*, 2001; *Sriver et al.,* 2008; *Jansen and Ferrari*, 2009; *Scoccimarro et al.,* 2011; *Manucharyan et al.,* 2011], in particular for past climate conditions exhibiting potentially higher levels of TC activity than the current climate [*Korty et al.,* 2008; *Fedorov et al.,* 2010].

Global observational estimates of TC-induced sea surface temperature (SST) anomalies indicate that the aggregated effect of these events is typically to cool the tropical oceans [*Cheng et al.,* 2015]. However, the characteristic temperature response in the northeastern Pacific region, South Indian Ocean, and other subtropical regions can be considerably different. Over the northeastern Pacific, for example, TCs tend to cause anomalous surface cooling within the southern portion of the region but anomalous warming in the northern portion, when integrated across all storms tracks annually [*Sriver and Huber*, 2007; *Sriver et al.,* 2008].

Here we quantify the aggregated effect of TC-induced surface heat fluxes on SST, using a suite of satellite-based and in situ observational products, along with results from a high-resolution Earth system model. We include in our analysis effects on top-of-the-atmosphere (TOA) radiation budgets, upper ocean

temperatures, and changes in cloudiness in the wake of storms. We focus primarily on explaining the observed temperature response in the northeastern Pacific region and discuss possible implications for local and global climate.

2. Methods

We analyze storm-induced changes in upper ocean temperatures, ocean-atmosphere fluxes, and cloud cover for all TCs globally during the period 2003–2013 using a best track data set that combines information from NOAA's Storm Prediction Center and the U.S. Navy's Joint Typhoon Warning Center. We employ a footprint method that samples storm properties within a 6×6 degree domain that is centered on the best track location and moves with each storm (as described in *Li et al.,* 2016). At each storm location, we analyze changes in SST, cloud fraction, and longwave and shortwave radiative fluxes. Anomalies are referenced either to local prestorm conditions (for temperature) or to climatological averages (for clouds and radiative fluxes). We use prestorm conditions for calculating temperature anomalies, because it preserves variability in the background conditions. Fluxes and clouds are referenced to the 10-year daily climatologies at each grid point, which enables us to compare conditions within storm wakes relative to typical non-storm conditions. The method assumes all anomalies are due to TC effects, and we neglect the effect of the seasonal cycle in the temperature anomaly calculations (which we assume to be small on the timescale of 1 week). We present all results as the long-term average of the annually aggregated effects.

Optimally interpolated (OI) SST data come from the Tropical Rainfall Measuring Mission's Microwave Imager (TMI) produced by Remote Systems Science with horizontal resolution of 0.25° [*Wentz*, 2015]. Satellite-derived products include top-of-atmosphere (TOA) radiative fluxes from NASA's Clouds and the Earth's Radiant Energy System (CERES) experiment [*Wielicki et al.,* 1996] and cloud properties from NASA's Moderate Resolution Imaging Spectroradiometer (MODIS). Subsurface ocean temperature data (from 2010 to 2013) are based on a weekly gridded Argo data product with 0.5×0.5 degree horizontal resolution [*Gaillard*, 2015] developed at the Laboratorie de Physique des Oceans and distributed by the Coriolis In Situ Service for Operational Oceanography. Monthly ocean mixed layer depth data (from 2000 to 2011) are obtained from the European Center for Medium-Range Weather Forecast Ocean Reanalysis System 4. Here mixed layer depth is defined by the 0.5°C temperature criterion.

The SST data retrieved by TMI may contain some biases at the edges of rain cells due to undetected rain. However, during the production of OI SST, some quality control was applied; particularly, SSTs greater than three standard deviations were flagged and removed from the data set. In addition, there are a few days when TMI observations were known to be missing; this, however, should not have a significant impact over a 10 year period (more information available at http://www.remss.com/measurements/sea-surface-temperature/oisst-description). For CERES TOA fluxes, *Su et al.* [2015] determined that the bias and root mean square error of the monthly mean TOA shortwave flux are less than 0.2 $W m^{-2}$ and 1.1 $W m^{-2}$, respectively, while the monthly mean TOA longwave flux is 0.5 $W m^{-2}$ and 0.8 $W m^{-2}$, respectively, both of which are over an order of magnitude smaller than the TC-induced anomalies. Lastly, this methodology for retrieval of cloud properties from MODIS was found to be robust and valuable for examining nonpolar regions [*Minnis et al.,* 2004].

To complement the observational analysis, we also examine modeled TC-ocean interactions using the Community Earth System Model (CESM) [*Hurrell et al.,* 2013]. CESM includes atmosphere, land surface, ocean, and sea ice model components, connected by a central coupler. To maintain methodological consistency with the observational analyses, we utilize 10 years of high-resolution model output from a fully coupled multidecadal CESM preindustrial control simulation. The simulation is configured with the 0.25° horizontal resolution Community Atmosphere Model version 5 (CAM5) [*Neale et al.*, 2010] with a spectral element dynamic core, coupled to the nominal 1° horizontal resolution ocean model (Parallel Ocean Program version 2) [*Smith et al.*, 2010]. The simulation is initialized with spun-up land surface conditions obtained from the National Center for Atmospheric Research (NCAR) (Jim Edwards, personal communication) and ocean conditions from the Polar Science Center Hydrographic Climatology ocean data set [*Levitus et al.,* 1998; *Steele et al.,* 2001]. While the coupled model simulation is not yet in full equilibrium, the 10-year period used in this study exhibits a near-balanced TOA radiation budget and relatively steady global-average surface temperature (Supporting Information Figure S1).

The simulated 10-year average SST pattern is generally consistent with observations, particularly within the tropics (Supporting Information Figure S2). We introduce several key changes to CESM to improve the representation of TC effects, including increased ocean-atmosphere coupling frequency to capture more realistic representation of near-inertial internal waves [*Jochum et al.,* 2013] and updated surface wind drag coefficient parameterization suitable for high wind regimes [*Moon et al.,* 2007]. The model generally simulates realistic TC climatologies (including number, seasonality and intensity distributions), as well as the transient upper ocean responses to TC forcing [*Li et al.,* 2016; *Li and Sriver*, 2016; *McClean et al.,* 2011]. The model exhibits some biases, such as reduced TC activity in the North Atlantic and relatively weak storms in the East Pacific (Supporting Information Figures S3 and S4). The suppressed TC activity is likely due to biases in seasonal SST and vertical wind shear over this region [*Li et al.,* 2016], which is an issue shared by other high-resolution coupled model simulations [*Small et al.,* 2014; *Kim et al.,* 2014].

Using the TC footprint method [*Li et al.,* 2016], we analyze TC-induced changes in cloudiness and SST/fluxes within observed and modeled storm wakes during the first week following the storms. We characterize storm-induced SST anomalies by following each storm track and subtracting the prestorm temperatures (-1 day relative to storm passage) from the poststorm temperatures (averaged from +3 to +5 days). We tested the sensitivity of the SST results to the choice of anomaly time frame and we chose to use +4 days because it represents the typical timing of the wake transition from the forced response to wake recovery stage [*Cheng et al.,* 2015]. Similarly, along each storm track, radiative fluxes and cloud fractions are calculated by subtracting the 10-year daily climatology from the storm-induced conditions for the period -1 to +4 days relative to storm passage and then averaging over the period.

3. Results

We find that TCs generally cool the surface ocean (Figure 1, Supporting Information Figure S5), and the magnitude of the cooling increases with TC activity (e.g., northwestern Pacific and northeastern Atlantic regions). The cooling is primarily due to vertical ocean mixing and, to a lesser extent, by enhanced surface evaporation [*Price*, 1981]. These regions also experience increased cloudiness associated with the storms (Figure 1f), which can potentially contribute to surface flux anomalies by reducing the amount of incoming solar radiation reaching the surface.

The average TC-induced SST response in the northeastern Pacific basin looks considerably different from other TC regions (Figure 1d). Here we find a strong dipole response in SST, with anomalous cooling in the southern portion of the basin and anomalous warming in the northern portion (statistically significant with p values less than 0.05—Supporting Information Figure S6). The areas of cooling and warming are separated roughly according to the location of the climatological 27°C isotherm of SST. Equatorward of the 27°C climatological isotherm, the anomalously cool region exhibits reduced downward heat fluxes and increased cloudiness consistent with other storm regions. These cool anomalies can persist for several weeks in this region [*Balaguru et al.,* 2014]. The response is opposite poleward of the 27°C isotherm. This anomalously warm region exhibits positive downward heat fluxes (Figure 1e) and decreased cloudiness (Figure 1f).

To identify the cause of the spatial variability in the northeastern Pacific, we isolate the individual heat flux contributions (Figure 2) and partition the cloud distributions into low- and high-level cloudiness. The southern portion experiences increased upward shortwave and decreased upward longwave fluxes (Figure 2), primarily due to enhanced storm clouds at high levels. The response is reversed in the northern region, and we conjecture the cause relates to regional differences in climatological SST and storm-induced changes in cloudiness. In northeastern Pacific areas cooler than 27°C, deep convection is suppressed, as shown by larger low-level cloudiness in the climatological cloud distributions and convective stability (Supporting Information Figure S7). We find that TCs tend to destroy these preexisting low-level clouds, enhancing convective mixing and stabilizing the lower atmosphere. This effect is stronger for higher intensity storms. The decreased poststorm low-level cloudiness in this region leads to increased surface shortwave radiation.

We also examined the potential contribution of ocean processes to the observed temperature dipole pattern using subsurface ocean temperatures from Argo floats and the high-resolution CESM simulation. Both the observations and the model show no indication of a temperature inversion in the northeastern Pacific

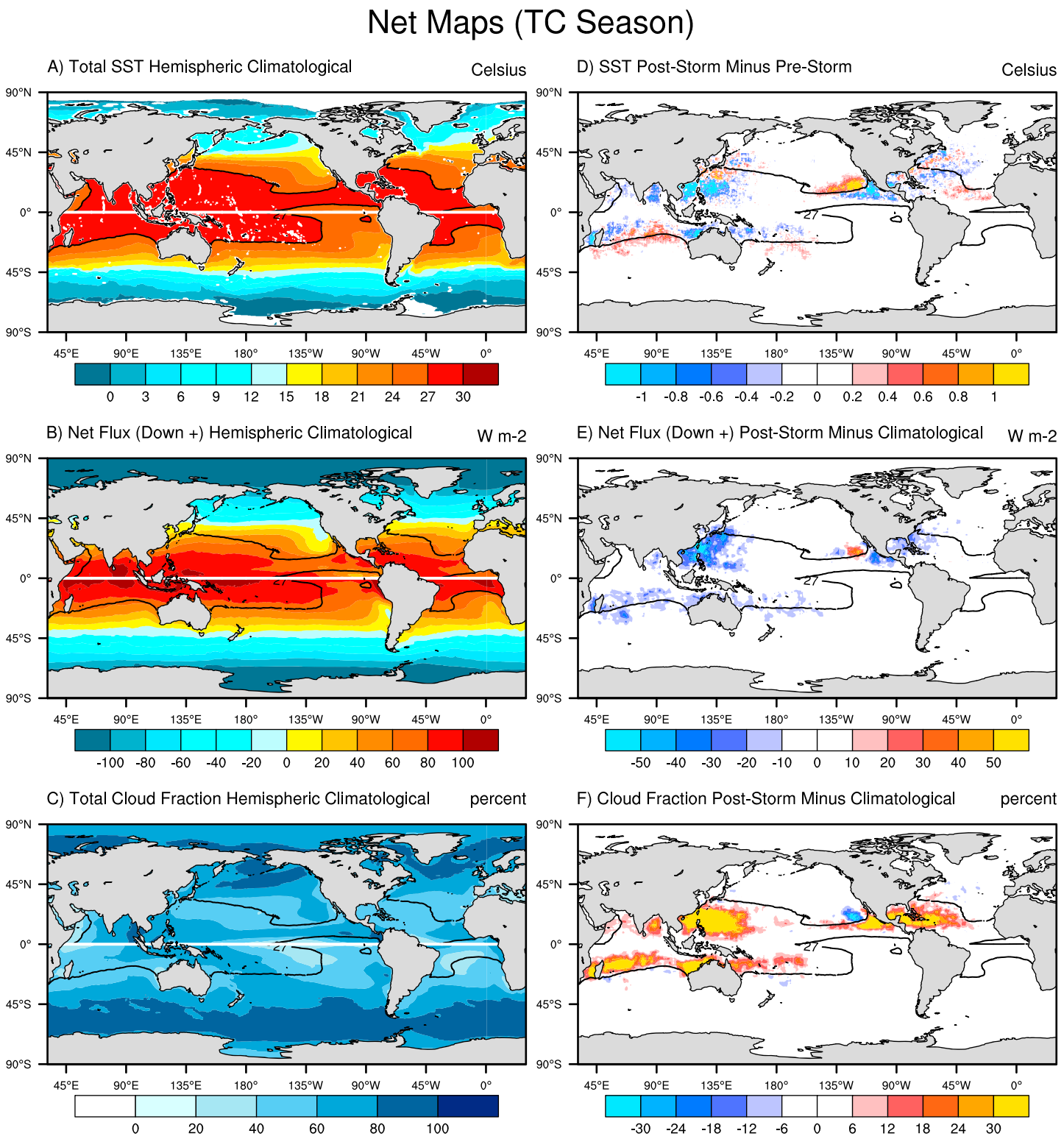

Figure 1. The impact of tropical cyclones in observations. (a) SST in °C, (b) net surface heat flux in W m^{-2}, and (c) total cloud fraction in percent, averaged over their respective hemisphere's TC season (hereafter, it is August to October for the northern hemisphere and February to April for the southern hemisphere) during the period 2003–2013. (D) Maps of TC-induced anomalous SST (averaged from +3 to +5 days poststorm minus −1 day prestorm), (e) net surface heat flux (storm-induced minus climatology), and (f) total cloud fraction (storm-induced minus climatology), calculated along storm tracks for the periods −1 to +4 days relative to storm passage. Black contour lines highlight the location of the 27°C isotherm from Figure 1a.

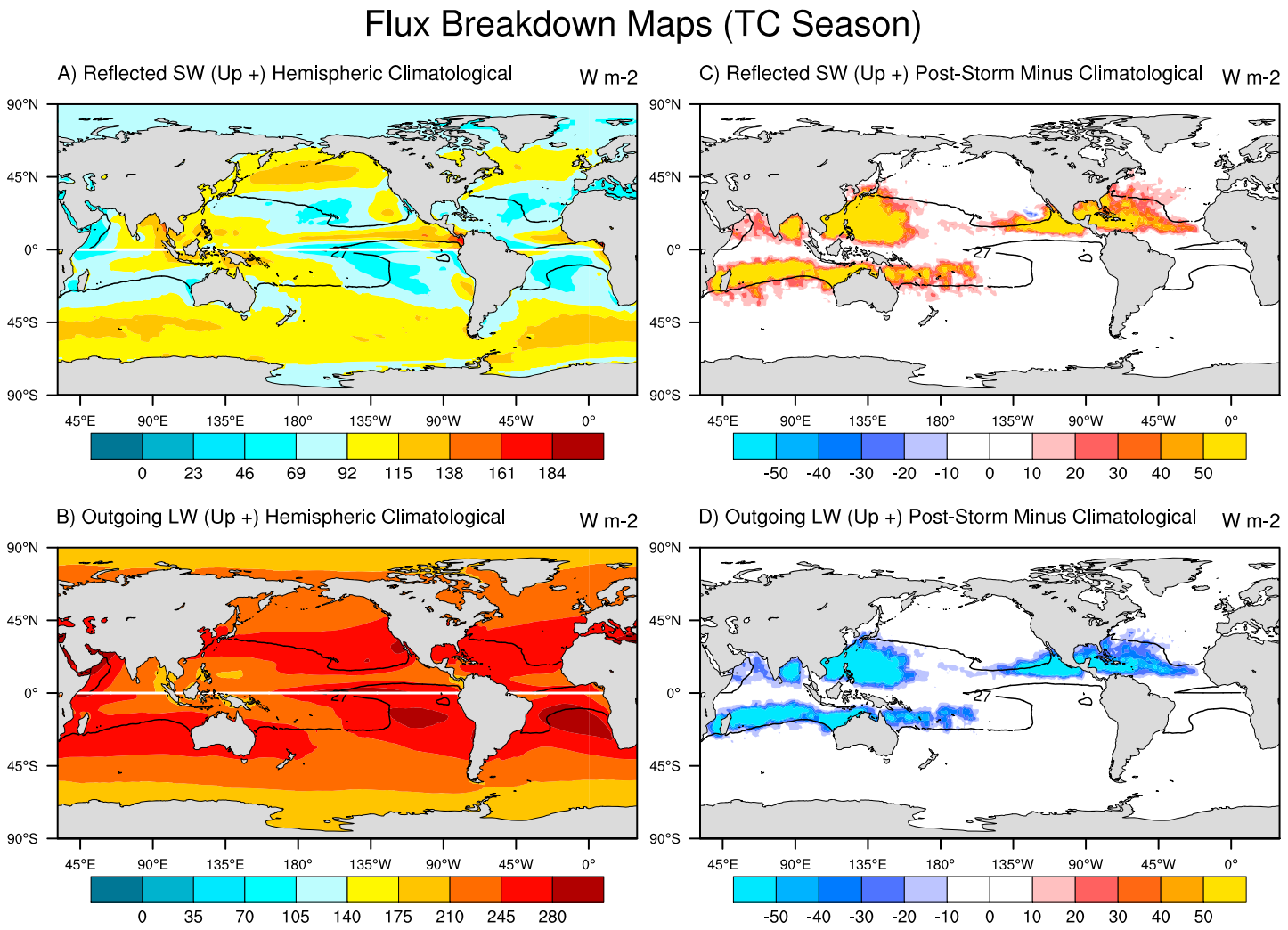

Figure 2. Observed of top-of-the-atmosphere fluxes. (a) The reflected shortwave radiation and (b) outgoing longwave radiation in W m^{-2}, averaged over their respective hemisphere's TC season during the period 2003–2013. (c) The TC-induced anomalous reflected shortwave radiation (storm-induced minus climatology) and (d) outgoing longwave radiation (storm-induced minus climatology) for the period 2003–2013. Anomalies are calculated along storm tracks for the periods −1 to +4 days relative to storm passage. Black contour lines highlight the location of the 27°C isotherm from Figure 1a.

based on the average vertical temperature profiles for the northern hemisphere TC season (Supporting Information Figure S8). However, the vertical temperature gradients are weaker, and deeper mixed layer depths are observed in the poleward region (Supporting Information Figure S9), suggesting weaker expected cooling by TC-induced vertical mixing compared to the equatorward region [*Balaguru et al.*, 2013]. The spatial variations in upper ocean heat content and mixed layer depth work in concert with the atmospheric shortwave forcing to induce the observed dipole response (Figure 3).

4. Discussion

Suppression of low clouds by TCs is not unique to the northeastern Pacific. Our analysis indicates that TCs can also reduce low-level cloudiness in several other regions inside or adjacent to the tropical ocean warm pool, such as the northwestern Pacific and south Indian Ocean. The South Indian Ocean experiences a nontrivial warming of about 0.5°C. Over this region there occurs a reduction in low clouds but increase in high clouds, which together may account for the surface warming. The northeastern Pacific represents the only region exhibiting the strong dipole pattern in the temperature response, which is in part due to the spatial distribution of low cloud coverage and the location of the seasonal 27°C isotherm.

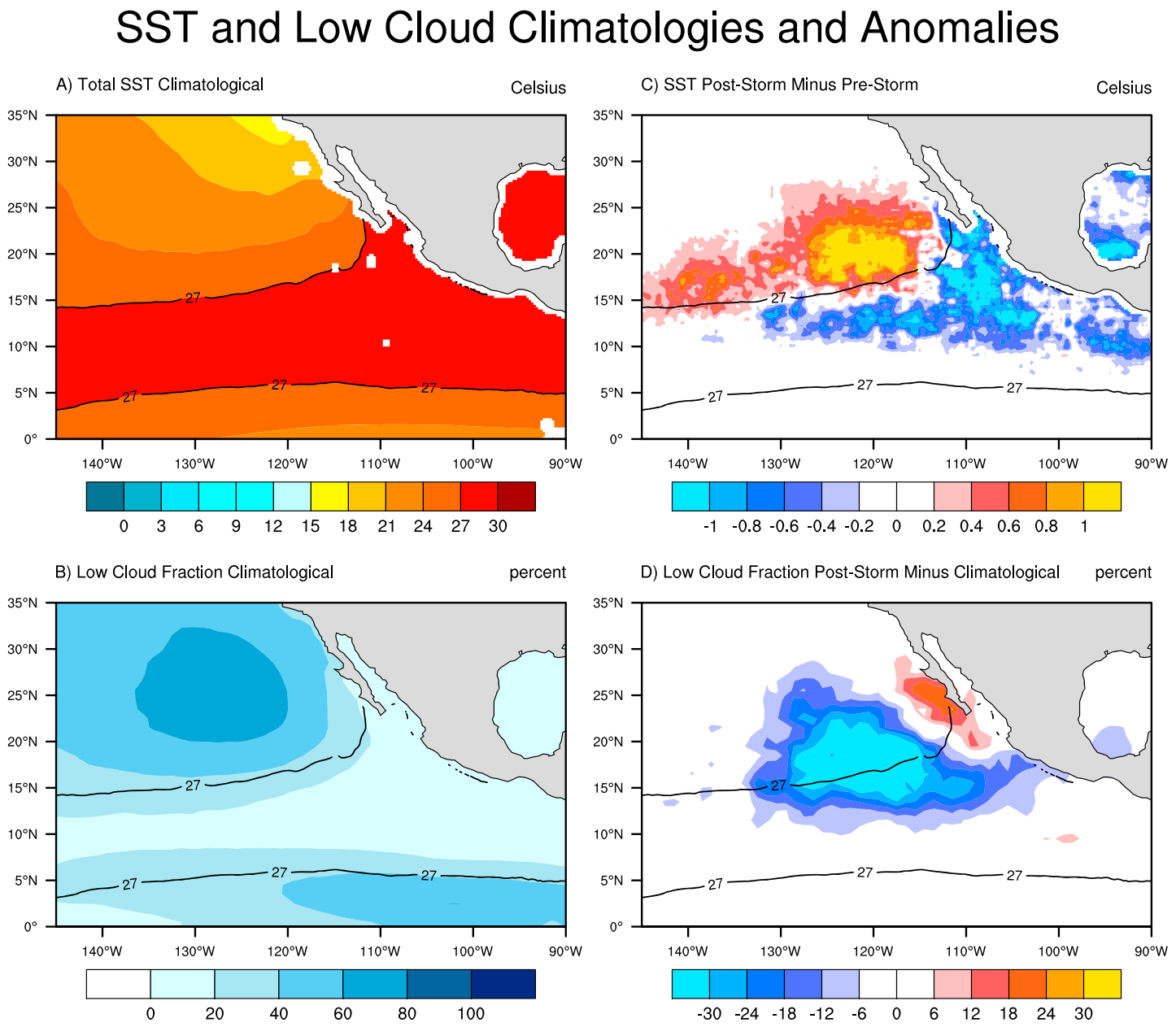

Figure 3. TC-induced ocean and cloud responses for the northeastern Pacific region. (a) Mean SST in °C and (b) low-level cloud fraction in percent averaged over the northern hemisphere TC season (August to October) during the period 2003–2013. (c) Annual averages of the TC-induced anomalous SST (poststorm minus prestorm) and (d) low-level cloud fraction (storm-induced minus climatology) for the period 2003–2013. Anomalies are calculated along storm tracks for the periods −1 to +4 days relative to storm passage. Black contour lines highlight the location of the 27°C isotherm from Figure 1a.

The observational results are generally replicated in the CESM simulation, which robustly captures the observed spatial patterns and variability in TC-induced SST anomalies and surface fluxes, including the dipole pattern in the northeastern Pacific region (Figure 4). Globally, the model overestimates the TC-induced ocean cooling, as compared to the observations, possibly masking some of the warming effects by enhanced radiative forcing. To investigate the amount of ocean warming induced by the poststorm fluxes in the northeastern Pacific, we use daily surface flux and ocean temperature output from CESM to compare TC-induced flux anomalies with anomalous ocean heat content during the 5 days immediately surrounding storm passage. We estimate TC-induced ocean heat content by integrating the storm-induced temperature anomalies along TC tracks (using the footprint method described previously) to 25 m depth, which represents the depth at which the warming anomaly goes to zero (Supporting Information Figure S10) [*Li et al.*, 2016; *Li and Sriver*,

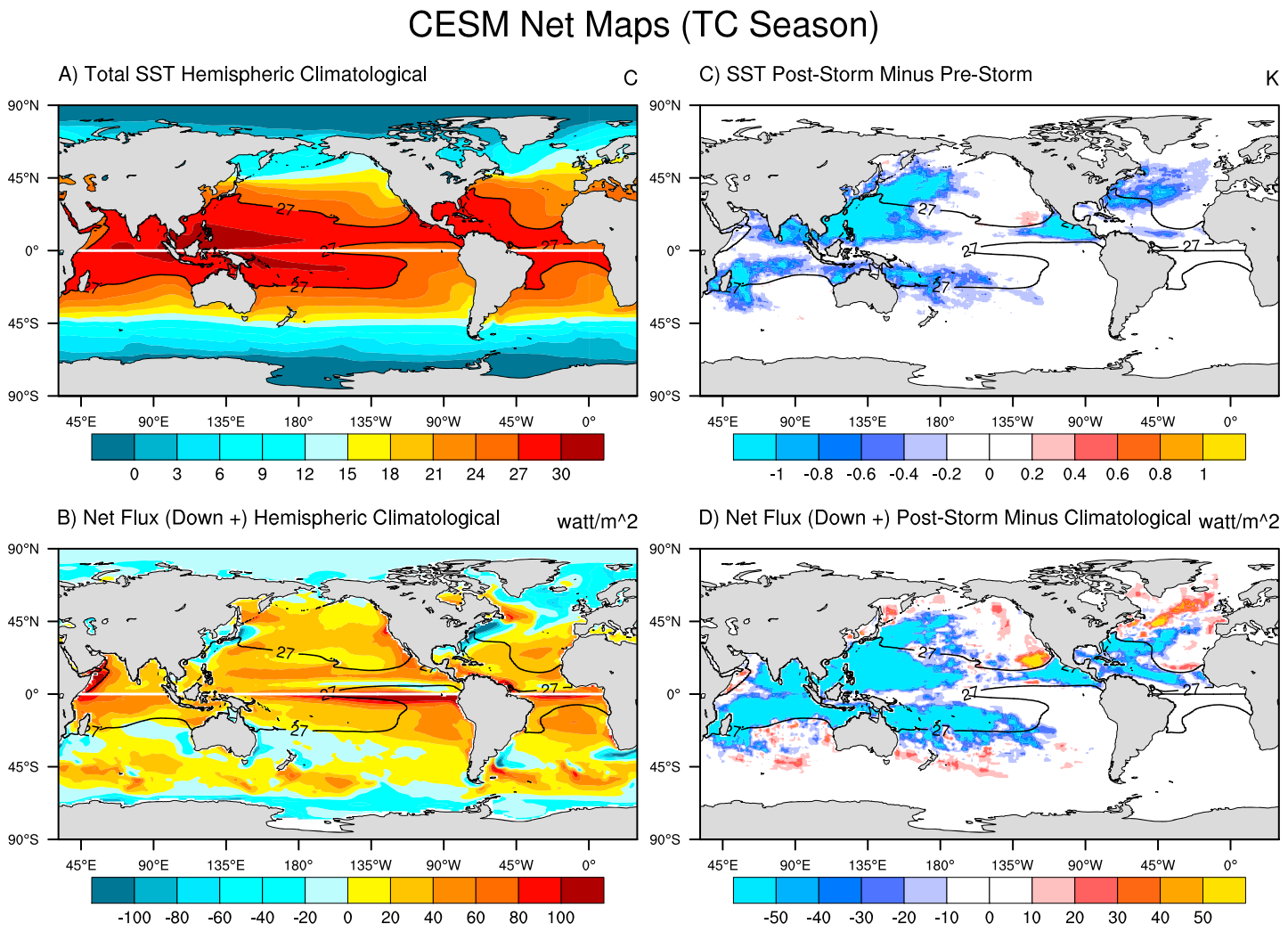

Figure 4. Simulated tropical cyclone impacts. (a) Maps of CESM's SST in °C and (b) net surface heat flux in W m^{-2}, averaged over their respective hemisphere's TC season during the period 2003–2013. (c) Maps of CESM's TC-induced anomalous SST (averaged from +3 to +5 days poststorm minus −1 day prestorm and (d) net surface heat flux (storm-induced minus climatology), calculated along storm tracks for the periods −1 to +4 days relative to storm passage. Black contour lines highlight the location of the 27°C isotherm from Figure 4a.

2016]. In the model, the annually aggregated anomalous ocean heat content in the uppermost 25 m (~0.20×10^8 J/km^2) is roughly consistent with the heating by TC-induced flux anomalies (~0.24×10^8 J/km^2) averaged over the northern TC region in the eastern Pacific.

The relationship between TCs, cloud cover, and surface fluxes may have important implications for surface heat budgets and tropical climate. On relatively short (weekly to monthly) timescales, these interactions can influence poststorm wake recoveries and potentially mask subsurface cooling by vertical mixing, which can in turn affect subsequent storm development and intensification. Moreover, the dipole response of the anomalous SST acts to reduce the background SST gradient in this region, with the potential to affect the weather patterns through modifications of near-surface baroclinicity and the subtropical jet stream.

On longer timescales, these results point to key climate connections between TC activity, SST patterns, cloud distributions, and surface radiation that could potentially influence the tropical mean state and variability. For example, it has been hypothesized that climates with enhanced TC-induced mixing may have been capable of sustaining permanent El Niño-like temperature patterns, exhibiting anomalously warm temperatures in the eastern equatorial Pacific region, such as during the early Pliocene (~5 million years ago; *Brierley et al.,*

2009). The positive feedback between TC activity and shortwave forcing in the northeastern Pacific region may have contributed to sustaining these climate conditions [*Fedorov et al.,* 2010]. Such feedbacks may have also been important for contributing to the warm Eocene conditions ~50 million years ago [e.g., *Korty et al.,* 2008].

Acknowledgments
The authors thank Kerry Emanuel for constructive comments and feedback on early versions of the manuscript. A.V. F. acknowledges grant support from NSF (AGS-1405272) and NOAA (NA14OAR4310277). R.L.S. and H.L. acknowledge support from the National Center for Supercomputing Applications (NCSA). This research is part of the Blue Waters sustained-petascale computing project, which is supported by the National Science Foundation (awards OCI-0725070 and ACI-1238993) and the state of Illinois. Blue Waters is a joint effort of the University of Illinois at Urbana-Champaign and its National Center for Supercomputing Applications. TMI data are produced by Remote Sensing Systems and sponsored by the NASA Earth Sciences Program. Data are available at www.remss.com. Cloud and radiation data: CERES data were obtained from the Atmospheric Science Data Center at the NASA Langley Research Center. Gridded Argo data were developed at the Laboratorie de Physique des Oceans and distributed by the Coriolis In Situ Service for Operational Oceanography. We also thank Kerry Emanuel for providing global TC best track data: http://eaps4.mit.edu/faculty/Emanuel/products.

References

Balaguru, K., L. R. Leung, and J.-H. Yoon (2013), Oceanic control of northeast pacific hurricane activity at interannual timescales, *Environ. Res. Lett.*, *8*, 044009, doi:10.1088/1748-9326/8/4/044009.

Balaguru, K., S. Taraphdar, L. R. Leung, G. R. Foltz, and J. A. Knaff (2014), Cyclone-cyclone interactions through the ocean pathway, *Geophys. Res. Lett.*, *41*, 6855–6862, doi:10.1002/2014GL061489.

Brierley, C. M., et al. (2009), Greatly expanded tropical warm pool and weakened Hadley circulation in the early Pliocene, *Science*, *323*, 1714–1718.

Bueti, M., I. Ginis, L. M. Rothstein, and S. M. Griffies (2014), Tropical cyclone-induced thermocline warming and its regional and global impacts, *J. Clim.*, *27*, 6978–6999, doi:10.1175/JCLI-D-14-00152.1.

Cheng, L., J. Zhu, and R. L. Sriver (2015), Global representation of tropical cyclone-induced short-term ocean thermal changes using Argo data, *Ocean Sci.*, *11*, 719–741, doi:10.5194/os-11-719-2015.

Emanuel, K. (2001), Contribution of tropical cyclones to meridional heat transport by the oceans, *J. Geophys. Res.*, *106*, 14,771–14,781, doi:10.1029/2000JD900641.

Fedorov, A. V., C. M. Brierley, and K. Emanuel (2010), Tropical cyclones and permanent El Niño in the early Pliocene epoch, *Nature*, *463*, 1066–U1084.

Gaillard, F. (2015), ISAS-13 temperature and salinity gridded fields Pôle Océan. [Available at http://doi.org/z77.]

Hart, R. E. (2011), An inverse relationship between aggregate northern hemisphere tropical cyclone activity and subsequent winter climate, *Geophys. Res. Lett.*, *38*, L01705, doi:10.1029/2010GL045612.

Hurrell, J. W., et al. (2013), The Community Earth System Model: A framework for collaborative research, *Bull. Am. Meteorol. Soc.*, *94*, 1339–1360.

Jansen, M., and R. Ferrari (2009), Impact of the latitudinal distribution of tropical cyclones on ocean heat transport, *Geophys. Res. Lett.*, *36*, L06604, doi:10.1029/2008GL036796.

Jansen, M. F., R. Ferrari, and T. A. Mooring (2010), Seasonal versus permanent thermocline warming by tropical cyclones, *Geophys. Res. Lett.*, *37*, L03602, doi:10.1029/2009GL041808.

Jochum, M., B. P. Briegleb, G. Danabasoglu, W. G. Large, N. J. Norton, S. R. Jayne, M. H. Alford, and F. O. Bryan (2013), The impact of oceanic near-inertial waves on climate, *J. Clim.*, *26*, 2833–2844, doi:10.1175/JCLI-D-12-00181.1.

Kim, H.-S., G. A. Vecchi, T. R. Knutson, W. G. Anderson, T. L. Delworth, A. Rosati, F. Zeng, and M. Zhao (2014), Tropical cyclone simulation and response to CO_2 doubling in the GFDL $CM_{2.5}$ high-resolution coupled climate model, *J. Clim.*, *27*(21), 8034–8054, doi:10.1175/JCLI-D-13-00475.1.

Korty, R. L., K. A. Emanuel, and J. R. Scott (2008), Tropical cyclone-induced upper-ocean mixing and climate: Application to equable climates, *J. Clim.*, *21*, 638–654, doi:10.1175/2007JCLI1659.1.

Levitus, S., T. P. Boyer, M. E. Conkright, D. Johnson, T. O'Brien, J. Antonov, C. Stephens, and R. Gelfeld (1998), *Introduction, vol. 1, World Ocean Database 1998, NOAA Atlas NESDIS 18*, pp. 346, U.S. Gov. Print. Off., Washington, D. C.

Li, H., and R. L. Sriver (2016), Effects of ocean grid resolution on TC-induced upper ocean responses using a global ocean general circulation model, *J. Geophys. Res. Oceans*, *121*, 8305–8319, doi:10.1002/2016JC011951.

Li, H., R. L. Sriver, and M. Goes (2016), Modeled sensitivity of the northwestern Pacific upper-ocean response to tropical cyclones in a fully-coupled climate model with varying ocean grid resolution, *J. Geophys. Res. Oceans*, *121*, 586–601, doi:10.1002/2015JC011226.

Manucharyan, G., C. Brierley, and A. V. Fedorov (2011), Climate impacts of intermittent ocean mixing induced by tropical cyclones, *J. Geophys. Res.*, *116*, C11038, doi:10.1029/2011JC007295.

McClean, J. L., et al. (2011), A prototype two-decade fully-coupled fine-resolution CCSM simulation, *Ocean Model.*, *39*(1–2), 10–30, doi:10.1016/j.ocemod.2011.02.011.

Mei, W., F. Primeau, J. C. McWilliams, and C. Pasquero (2013), Sea surface height evidence for long-term warming effects of tropical cyclones on the ocean, *Proc. Natl. Acad. Sci. U.S.A.*, *110*, 15,207–15,210, doi:10.1073/pnas.1306753110.

Minnis, P., D. F. Young, S. Sun-Mack, P. W. Heck, D. R. Doelling, and Q. Z. Trepte (2004), CERES Cloud Property Retrievals from Imagers on TRMM, Terra, and Aqua, 5235:37–48. doi:10.1117/12.511210.

Moon, I.-J., I. Ginis, T. Hara, and B. Thomas (2007), A physics-based parameterization of air–sea momentum flux at high wind speeds and its impact on hurricane intensity predictions, *Mon. Weather Rev.*, *135*(8), 2869–2878, doi:10.1175/MWR3432.1.

Neale, R. B., et al. (2010), Description of the NCAR community atmosphere model (CAM 5.0), NCAR Tech. Note NCAR/TN-4861 STR. Natl. Cent. Atmos. Res., Boulder, Colo.

Pasquero, C., and K. Emanuel (2008), Tropical cyclones and transient upper-ocean warming, *J. Clim.*, *21*, 149–162, doi:10.1175/2007JCLI1550.1.

Price, J. F. (1981), Upper ocean response to a hurricane, *J. Phys. Oceanogr.*, *11*(153–175), 1981.

Scoccimarro, E., S. Gualdi, A. Bellucci, A. Sanna, P. Giuseppe Fogli, E. Manzini, M. Vichi, P. Oddo, and A. Navarra (2011), Effects of tropical cyclones on ocean heat transport in a high-resolution coupled general circulation model, *J. Clim.*, *24*, 4368–4384, doi:10.1175/2011JCLI4104.1.

Small, R. J., et al. (2014), A new synoptic scale resolving global climate simulation using the Community Earth System Model, *J. Adv. Model. Earth Syst.*, *6*(4), 1065–1094, doi:10.1002/2014MS000363.

Smith, R. D., et al. (2010), The Parallel Ocean Program (POP) reference manual, Tech. Rep. LAUR-10-01853, Los Alamos Natl. Lab., Los Alamos, N. M.

Sriver, R. L., and M. Huber (2007), Observational evidence for an ocean heat pump induced by tropical cyclones, *Nature*, *447*, 577–580, doi:10.1038/nature05785.

Sriver, R. L., and M. Huber (2010), Modeled sensitivity of upper thermocline properties to tropical cyclone winds and possible feedbacks on the Hadley circulation, *Geophys. Res. Lett.*, *37*, L08704, doi:10.1029/2010GL042836.

Sriver, R. L., M. Huber, and J. Nusbaumer (2008), Investigating tropical cyclone-climate feedbacks using the TRMM Microwave Imager and the Quick Scatterometer, *Geochem., Geophys., Geosyst.*, *9*, Q09V11, doi:10.1029/2007GC001842.

Sriver, R. L., M. Goes, M. E. Mann, and K. Keller (2010), Climate response to tropical cyclone-induced ocean mixing in an Earth system model of intermediate complexity, *J. Geophys. Res.*, *115*, C10042, doi:10.1029/2010JC006106.

Steele, M., R. Morley, and W. Ermold (2001), PHC: A global ocean hydrography with a high-quality Arctic Ocean, *J. Clim.*, *14*(9), 2079–2087, doi:10.1175/1520-0442(2001)014<2079:PAGOHW>2.0.CO;2.

Su, W., J. Corbett, Z. Eitzen, and L. Liang (2015), Next-generation angular distribution models for top-of-atmosphere radiative flux calculation from CERES instruments: Validation, *Atmos. Meas. Tech.*, *8*(8), 3297–3313, doi:10.5194/amt-8-3297-2015.

Wentz, F. J. (2015), A 17-yr climate record of environmental parameters derived from the Tropical Rainfall Measuring Mission (TRMM) Microwave Imager, *J. Clim.*, *28*, 6882–6902, doi:10.1175/JCLI-D-15-0155.1.

Wielicki, B. A., B. R. Barkstrom, E. F. Harrison, R. B. Lee III, G. L. Smith, and J. E. Cooper (1996), Clouds and the Earth's Radiant Energy System (CERES): An Earth observing system experiment, *Bull. Am. Meteorol. Soc.*, *77*, 853–868.